

Supplementary Material

Detailed *in vitro* pharmacological characterization of clinically tested negative allosteric modulators of the metabotropic glutamate receptor 5 (mGlu₅)

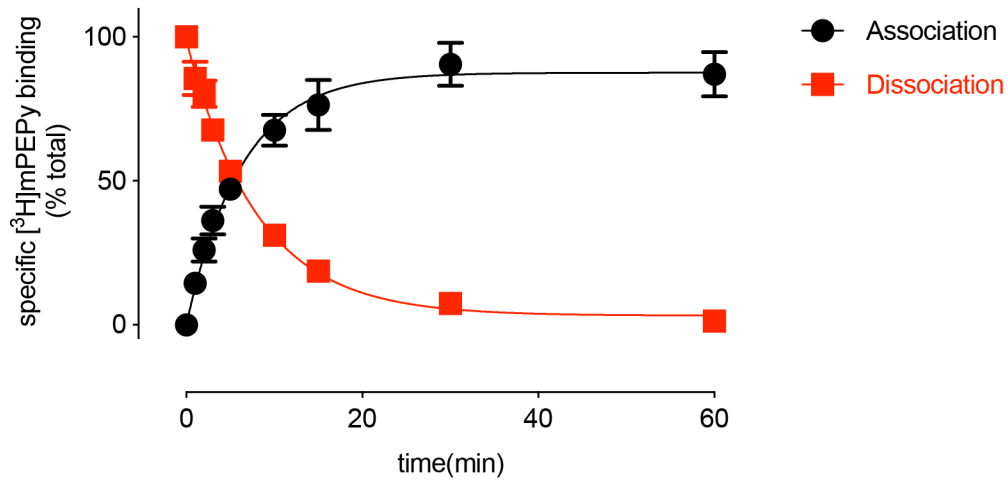
Angela Arsova^a, Thor C. Møller^a, Line Vedel^a, Jakob Lerche Hansen^c, Simon R. Foster^a, Karen Gregory^{b*} & Hans Bräuner-Osborne^{a*}

^a *Department of Drug Design and Pharmacology, Faculty of Health and Medical Sciences, University of Copenhagen, Universitetsparken 2, 2100 Copenhagen, Denmark*

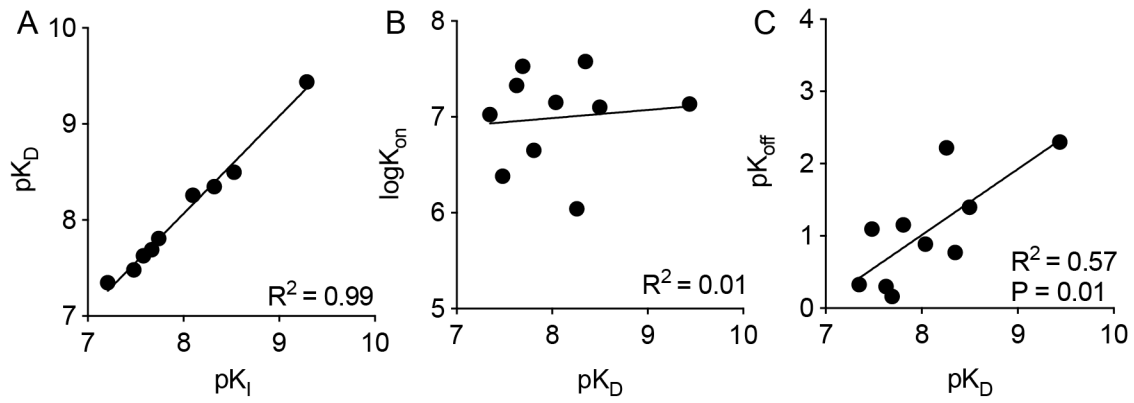
^b *Drug Discovery Biology, Monash Institute of Pharmaceutical Sciences and Department of Pharmacology, Monash University, Parkville, VIC, Australia*

^c *Cardiovascular Research, Novo Nordisk A/S, Novo Nordisk Park 1, 2760 Måløv, Denmark*

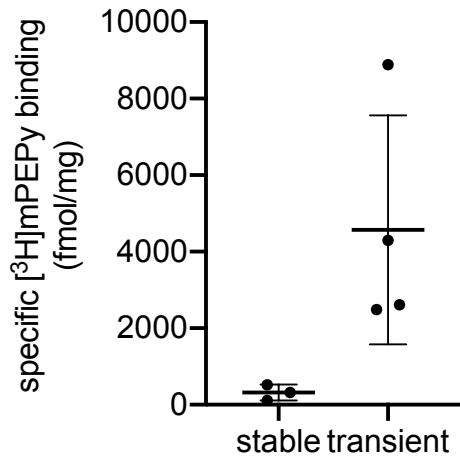
* *Contributed equally to this work. Correspondence and requests for materials should be addressed to K.J.G. (email: karen.gregory@monash.edu) or H.B.-O. (email: hbo@sund.ku.dk)*



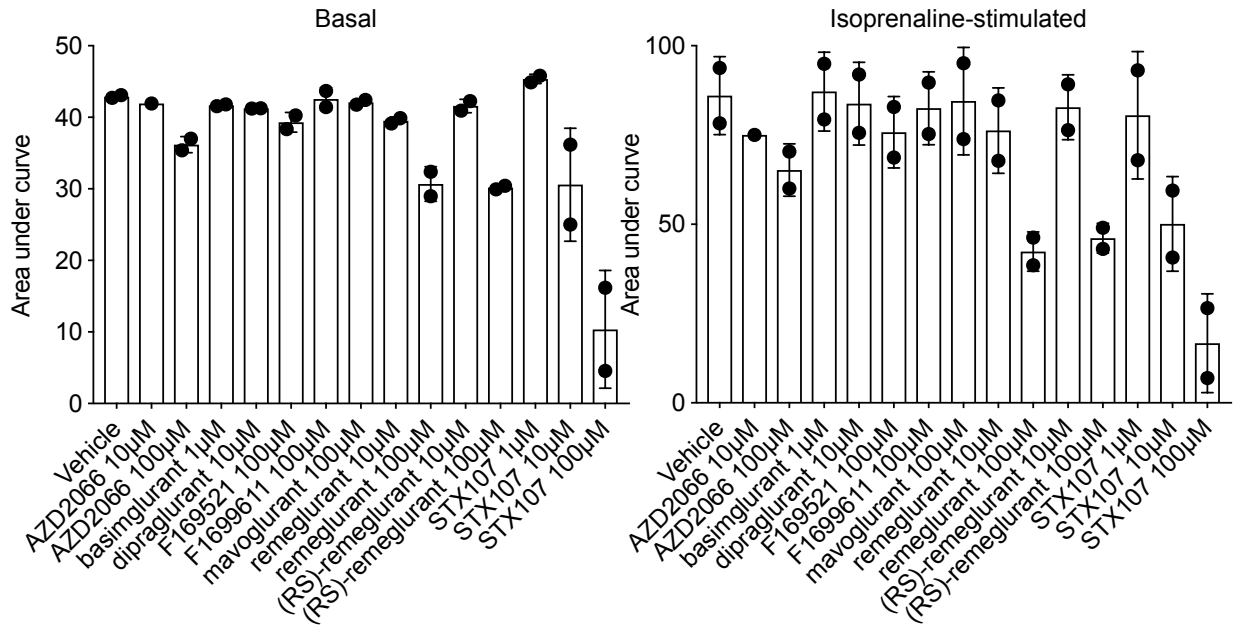
Supplementary Figure 1. Association and dissociation kinetics of [³H]methoxy-PEPy binding in HEK293A-mGlu₅-low cell membranes. The dissociation rate was determined by simultaneous addition of a saturating concentration of unlabeled competitive ligand (1 μM MPEP). Data are represented as mean ± SEM of 7 independent experiments performed in duplicate. Error bars not shown lie within the dimensions of the symbol.



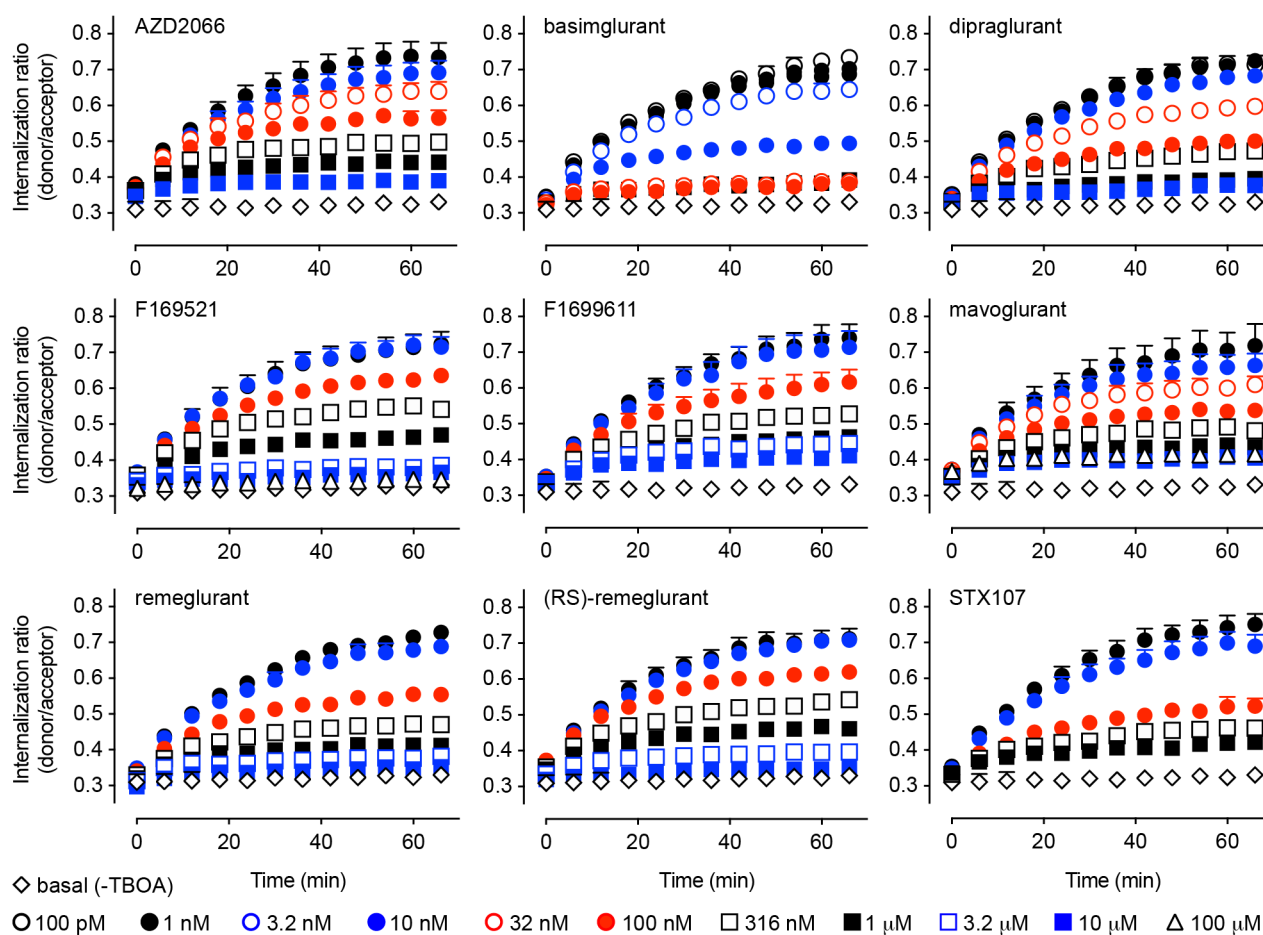
Supplementary Figure 2. Correlation plots of affinity, association rate, and dissociation rate of mGlu₅ NAMs. **A)** Affinities calculated from association (k_{on}) and dissociation (k_{off}) rates ($K_D = k_{off}/k_{on}$), where pK_D is the negative logarithm of K_D , versus pK_I estimates from inhibition binding experiments. **B)** Association rates do not correlate with pK_D . **C)** Dissociation rates correlate with pK_D .



Supplementary Figure 3. B_{\max} estimates for [^3H]mPEPy binding to mGlu $_5$ in membranes from stable and transient transfected HEK293A cells. To estimate total receptor levels (B_{\max}), two-point saturation binding experiments were performed using 2.6 ± 1.1 nM and 16.6 ± 3.6 nM [^3H]mPEPy and 10 μM MPEP to define non-specific binding. A saturation binding isotherm was fitted to the data to estimate B_{\max} , with the assumption that the N-terminal SNAP-tag had no effect on the affinity of the allosteric radioligand ([^3H]mPEPy, reported in Table 1), which binds to the 7TM domain. Independent replicates for $n=3-4$ are shown, data are mean \pm SD.



Supplementary Figure 4. High concentrations of select mGlu₅ NAMs interfere with FRET-based assay detection. The basal and agonist (isoprenaline)-stimulated internalization of SNAP-tagged β_2 -adrenoceptor measured in presence of high concentrations of mGlu₅ NAMs or vehicle (1% DMSO). Area under the curve was calculated for real time internalization ratios (ratio of donor and acceptor emissions) measured for 66 min in 6 min intervals. Data points represent the mean of individual experiments and bars represent mean \pm SEM from two independent experiments performed in triplicate.



Supplementary Figure 5. Real-time mGlu₅ internalization in response to 11.6 μM of L-glutamate is inhibited by mGlu₅ NAMs. Indicated NAMs were pre-incubated for 30 min prior to addition of L-glutamate (11.6 μM), fluorescein and DL-TBOA (to inhibit transport of glutamate). The ratio of donor (Lumi4-Tb-labeled SNAP-tagged mGlu₅) and acceptor (fluorescein) emissions (internalization ratio) increases over time when the receptor is internalized. Data are mean + SEM from 3 independent experiments performed in triplicate.

Supplementary Table 1: L-glutamate potency for mGlu₅ in four functional assays. Data are represented as mean ± SEM from the indicated number (n) of independent experiments performed in triplicate.

	pEC ₅₀	n
Ca ²⁺ mobilization	6.53±0.13	4
IP ₁ accumulation	5.40±0.05	5
ERK1/2 phosphorylation	6.00±0.05	4
Receptor internalization	5.47±0.08	3
	5.80±0.19 [#]	

[#] For receptor internalization data the concentration-response curve was re-fitted such that the bottom plateau was equal to the true basal level of the system, i.e. in the absence of DL-TBOA. In order to do so, the data points below the inflection point of the original curve were removed (100 nM and 1 μM).

Supplementary Table 2: Potency (pIC₅₀) values from functional assays for mGlu₅ NAMs, based on titrations in the presence of sub-maximal L-glutamate. Data was fitted to a four-parameter model of inhibition. Values are mean ± SEM from the indicated number (n) of independent experiments performed in triplicate.

	Ca²⁺ mobilization		IP₁ accumulation		ERK1/2 phosphorylation		Receptor internalization	
	pIC₅₀	n	pIC₅₀	n	pIC₅₀	n	pIC₅₀	n
AZD2066	7.29 ± 0.33	4	8.52 ± 0.04	4	7.88 ± 0.09	3	6.85 ± 0.03	3
basimglurant	9.13 ± 0.16	4	9.42 ± 0.07	4	8.99 ± 0.06	4	8.12 ± 0.04	3
dipraglurant	6.44 ± 0.20	4	7.37 ± 0.04	4	6.93 ± 0.12	3	7.14 ± 0.02	3
F169521	6.69 ± 0.12	4	7.07 ± 0.06	4	6.83 ± 0.03	3	6.34 ± 0.06	3
F1699611	7.16 ± 0.31	4	7.71 ± 0.10	4	7.21 ± 0.11	3	6.77 ± 0.10	3
mavoglurant	7.22 ± 0.27	4	8.43 ± 0.07	4	7.62 ± 0.05	3	7.09 ± 0.12	3
remeglurant	6.96 ± 0.29	4	7.92 ± 0.13	4	7.38 ± 0.14	3	6.78 ± 0.05	3
(RS)-remeglurant	6.63 ± 0.26	4	7.20 ± 0.04	4	7.00 ± 0.10	3	6.22 ± 0.05	3
STX107	7.81 ± 0.25	4	8.44 ± 0.08	4	8.00 ± 0.04	3	7.29 ± 0.09	3